

Noise improvement of SNR gain in parallel array of bistable dynamic systems by array stochastic resonance

Fabing Duan *

Institute of Complexity Science, Qingdao University, Qingdao 266071, People's Republic of China

François Chapeau-Blondeau †

Laboratoire d'Ingénierie des Systèmes Automatisés (LISA), Université d'Angers,

62 avenue Notre Dame du Lac, 49000 Angers, France

Derek Abbott ‡

Centre for Biomedical Engineering (CBME) and School of Electrical & Electronic Engineering,

The University of Adelaide, SA 5005, Australia

April 13, 2021

Abstract

We report the regions where a signal-to-noise ratio (SNR) gain exceeding unity exists in a parallel uncoupled array of identical bistable systems, for both subthreshold and suprathreshold sinusoids buried in broadband Gaussian white input noise. Due to independent noise in each element of the parallel array, the SNR gain of the collective array response approaches its local maximum exhibiting a stochastic resonant behavior. Moreover, the local maximum SNR gain, at a non-zero optimal array noise intensity, increases as the array size rises. This leads to the conclusion of the global maximum SNR gain being obtained by an infinite array. We suggest that the performance of infinite arrays can be closely approached by an array of *two* bistable oscillators operating in different noisy conditions, which indicates a simple but effective realization of arrays for improving the SNR gain. For a given input SNR, the optimization of maximum SNR gains is touched upon in infinite arrays by tuning both array noise levels and an array parameter. The nonlinear collective phenomenon of SNR gain amplification in parallel uncoupled dynamical arrays, i.e. array stochastic resonance, together with the possibility of the SNR gain exceeding unity, represent a promising application in array signal processing.

1 Introduction

The past decade has seen a growing interest in the research of stochastic resonance (SR) phenomena in interdisciplinary fields, involving physics, biology, neuroscience, and information processing. Conventional SR has usually been defined in terms of a metric such as the output signal-to-noise ratio (SNR) being a non-monotonic function of the background noise intensity, in a nonlinear (static or dynamic) system driven by a subthreshold periodic input [1]. For more general inputs, such as non-stationary, stochastic, and broadband signals, adequate SR quantifiers are information-theoretic measures [1, 2]. Furthermore, aperiodic SR represents a new form of SR dealing with aperiodic inputs [3]. The coupled array of dynamic elements

*fabing1974@yahoo.com.cn

†chapeau@univ-angers.fr

‡dabbott@eleceng.adelaide.edu.au

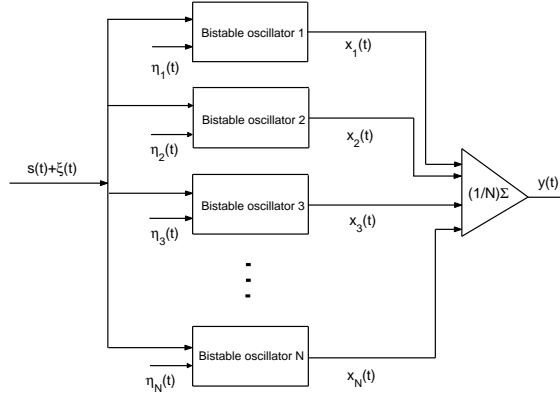


Figure 1: A parallel array of N archetypal over-damped bistable oscillators. Each oscillator is subject to the same noisy signal but independent array noise. In this paper, we call $\xi(t)$ the input noise and $\eta_i(t)$ the array noise.

[4, 5, 6, 7] and spatially extended systems [8] have been investigated not only for optimal noise intensity but also for optimal coupling strength, leading to the global nonlinear effect of spatiotemporal SR [8]. By contrast, the parallel uncoupled array of nonlinear systems gives rise to the significant feature that the overall response of the system depends on both subthreshold and suprathreshold inputs [9, 10, 11, 12, 13, 14, 15, 16, 17, 18, 19]. In this way, a novel form of SR, termed suprathreshold SR [12], attracted much attention in the area of noise-induced information transmissions, where the input signals are suprathreshold for the threshold of static systems or the potential barrier of dynamic systems [12, 13, 14, 15, 16, 17, 18, 19]. In addition, for a single bistable system, residual SR (or aperiodic SR) effects are observed in the presence of slightly suprathreshold periodic (or aperiodic) inputs [20, 21].

So far, the measure most frequently employed for conventional (periodic) SR is the SNR [1, 2, 22]. The SNR gain defined as the ratio of the output SNR over the input SNR, also attracts much interest in exploring situations where it can exceed unity [28, 29, 30, 31, 19, 32, 33, 2, 34, 35, 36, 37, 38, 39]. Within the regime of validity of linear response theory, it has been repeatedly pointed out that the gain cannot exceed unity for a nonlinear system driven by a sinusoidal signal and Gaussian white noise [23, 24, 25, 26, 27]. However, beyond the regime where linear response theory applies, it has been demonstrated that the gain can indeed exceed unity in non-dynamical systems, such as a level-crossing detector [28], a static two-threshold nonlinearity [29, 30, 31], and parallel arrays of threshold comparators or sensors [19, 32, 33], and also in dynamical systems, for instance, a single bistable oscillator [2, 34, 35, 36, 37, 38, 39], a non-hysteretic rf superconducting quantum interference device (SQUID) loop [40], and a global coupled network [5].

A pioneering study of a parallel uncoupled array of bistable oscillators has been performed with a general theory based on linear response theory [26], wherein the SNR gain is below unity. Recently, Casado *et al* reported that the SNR gain is larger than unity for a mean-field coupled set of noisy bistable subunits driven by subthreshold sinusoids [7]. However, each bistable subunit is subject to a *net* sinusoidal signal without input noise. The conditions yielding a SNR gain exceeding unity have not been touched upon in a parallel uncoupled array of bistable oscillators, in the presence of either a subthreshold or suprathreshold sinusoid and Gaussian white noise. In practice, an initially given noisy input is often met, and a signal processor operating under this condition, with the feature of the SNR gain exceeding unity, will be of interest [32, 33]. The SNR gain has been studied earlier in the less stringent condition of narrowband noise [41]. In the present paper, we address the more stringent condition of broadband white noise and the SNR gain achievable by summing the array output, wherein extra array noise can be tuned to maximize the array SNR gain. As the

array size is equal to or larger than two, the array SNR gain follows a SR-type function of the array noise intensity. More interestingly, the regions where the array SNR gain can exceed unity for a moderate array size, are demonstrated numerically for both subthreshold and suprathreshold sinusoids. Since the array SNR gain is amplified as the array size increases from two to infinity, we can immediately conclude that an infinite parallel array of bistable oscillators has a global maximum array SNR gain for a fixed noisy sinusoid. For an infinite parallel array, a tractable approach is proposed using an array of two bistable oscillators, in view of the functional limit of the autocovariance function [43]. We note that, for obtaining the maximum array SNR gain, the control of this new class of array SR effect focuses on the addition of array noise, rather than the input noise. This approach can also overcome a difficult case confronted by the conventional SR method of adding noise. When the initial input noise intensity is beyond the optimal point corresponding to the SR region of the nonlinear system, the addition of more noise will only worsen the performance of system [42]. Finally, the optimization of the array SNR gain in an infinite array is touched upon by tuning both an array parameter and array noise, and an optimal array parameter is expected to obtain the global maximum array SNR gain. These significant results indicate a series of promising applications in array signal processing in the context of array SR effects.

2 The model and the array SNR gain

The parallel uncoupled array of N archetypal over-damped bistable oscillators is considered as a model, as shown in Fig. 1. Each bistable oscillator is subject to the same signal-plus-noise mixture $s(t) + \xi(t)$, where $s(t) = A \sin(2\pi t/T_s)$ is a deterministic sinusoid with period T_s and amplitude A , and $\xi(t)$ is zero-mean Gaussian white noise, independent of $s(t)$, with autocorrelation $\langle \xi(t)\xi(0) \rangle = D_\xi \delta(t)$ and noise intensity D_ξ . At the same time, zero-mean Gaussian white noise $\eta_i(t)$, together with and independent of $s(t) + \xi(t)$, is applied to each element of the parallel array of size N . The N array noise terms $\eta_i(t)$ are mutually independent and have autocorrelation $\langle \eta_i(t)\eta_i(0) \rangle = D_\eta \delta(t)$ with a same noise intensity D_η [33]. The internal state $x_i(t)$ of each dynamic bistable oscillator is governed by

$$\tau_a \frac{dx_i(t)}{dt} = x_i(t) - \frac{x_i^3(t)}{X_b^2} + s(t) + \xi(t) + \eta_i(t), \quad (1)$$

for $i = 1, 2, \dots, N$. Their outputs, as shown in Fig. 1, are averaged and the response of the array is given as

$$y(t) = \frac{1}{N} \sum_{i=1}^N x_i(t). \quad (2)$$

Here, the real tunable array parameters τ_a and X_b are in the dimensions of time and amplitude, respectively [21]. We now rescale the variables according to

$$x_i(t)/X_b \rightarrow x_i(t), \quad A/X_b \rightarrow A, \quad t/\tau_a \rightarrow t, \quad T_s/\tau_a \rightarrow T_s, \quad D_\xi/(\tau_a X_b^2) \rightarrow D_\xi, \quad D_\eta/(\tau_a X_b^2) \rightarrow D_\eta, \quad (3)$$

where each arrow points to a dimensionless variable. Equation (1) is then recast in dimensionless form as,

$$\frac{dx_i(t)}{dt} = x_i(t) - x_i^3(t) + s(t) + \xi(t) + \eta_i(t). \quad (4)$$

Note that $s(t)$ is subthreshold if the dimensionless amplitude $A < A_c = 2/\sqrt{27} \approx 0.385$, otherwise it is suprathreshold [2, 21].

In general, the summed output response of arrays $y(t) = (1/N) \sum_{i=1}^N x_i(t)$ is a random signal. However, since $s(t)$ is periodic, $y(t)$ will in general be a cyclostationary random signal with the same period T_s [31]. A generalized theory has been proposed for calculating the output SNR [31]. According to the theory in [31], the summing response of arrays $y(t)$, at

any time t , can be expressed as the sum of its nonstationary mean $E[y(t)]$ plus the statistical fluctuations $\tilde{y}(t)$ around the mean $E[y(t)]$, as

$$y(t) = \tilde{y}(t) + E[y(t)]. \quad (5)$$

The nonstationary mean $E[y(t)] = (1/N) \sum_{i=1}^N E[x_i(t)]$ is a deterministic periodic function of time t with period T_s , having the order n Fourier coefficient

$$\bar{Y}_n = \left\langle E[y(t)] \exp(-i2\pi \frac{n}{T_s} t) \right\rangle, \quad (6)$$

where $\langle \dots \rangle = (1/T_s) \int_0^{T_s} \dots dt$. For fixed t and τ , the expectation $E[y(t)y(t+\tau)]$ is given by

$$E[y(t)y(t+\tau)] = E[\tilde{y}(t)\tilde{y}(t+\tau)] + E[y(t)]E[y(t+\tau)]. \quad (7)$$

Then, the stationary autocorrelation function $R_{yy}(\tau)$ for $y(t)$ can be calculated by averaging $E[y(t)y(t+\tau)]$ over the period T_s , as

$$\begin{aligned} R_{yy}(\tau) &= \langle E[y(t)y(t+\tau)] \rangle \\ &= \langle E[\tilde{y}(t)\tilde{y}(t+\tau)] \rangle + \langle E[y(t)]E[y(t+\tau)] \rangle \\ &= C_{yy}(\tau) + \langle E[y(t)]E[y(t+\tau)] \rangle, \end{aligned} \quad (8)$$

with the stationary autocovariance function $C_{yy}(\tau)$ of $y(t)$. The power spectral density $P_{yy}(\nu)$ of $y(t)$ is the Fourier transform of the autocorrelation function $R_{yy}(\tau)$

$$\begin{aligned} P_{yy}(\nu) &= \mathcal{F}[R_{yy}(\tau)] = \int_{-\infty}^{+\infty} R_{yy}(\tau) \exp(-i2\pi\nu\tau) d\tau \\ &= \mathcal{F}[C_{yy}(\tau)] + \sum_{n=-\infty}^{+\infty} \bar{Y}_n \bar{Y}_n^* \delta(\nu - \frac{n}{T_s}). \end{aligned} \quad (9)$$

It is seen that the power spectral density $P_{yy}(\nu)$ is formed by spectral lines with magnitude $|\bar{Y}_n|^2$ at coherent frequencies n/T_s , superposed to a broadband noise background represented by the Fourier transform of $C_{yy}(\tau)$. Note that $E[\tilde{y}(t)\tilde{y}(t)] = \text{var}[y(t)]$ represents the nonstationary variance of $y(t)$, which, after time averaging over a period T_s , leads to $C_{yy}(0) = \langle \text{var}[y(t)] \rangle$, the stationary variance of $y(t)$. The deterministic function $C_{yy}(\tau)$ can thus be expressed as

$$C_{yy}(\tau) = \langle \text{var}[y(t)] \rangle h(\tau), \quad (10)$$

where the correlation coefficient $h(\tau)$ is a deterministic even function describing the normalized shape of $C_{yy}(\tau)$, having a Fourier transform $\mathcal{F}[h(\tau)] = H(\nu)$. The power spectral density of Eq. (9) can then be rewritten as

$$P_{yy}(\nu) = \langle \text{var}[y(t)] \rangle H(\nu) + \sum_{n=-\infty}^{+\infty} \bar{Y}_n \bar{Y}_n^* \delta(\nu - \frac{n}{T_s}). \quad (11)$$

The output SNR is defined as the ratio of the power contained in the output spectral line at the fundamental frequency $1/T_s$ and the power contained in the noise background in a small frequency bin ΔB around $1/T_s$, i.e.

$$R_{\text{out}}(1/T_s) = \frac{|\bar{Y}_1|^2}{\langle \text{var}[y(t)] \rangle H(1/T_s) \Delta B}. \quad (12)$$

In addition, the output noise is a Lorentz-like colored noise with the correlation time τ_r defined by

$$h(|\tau| \geq \tau_r) \leq 0.05. \quad (13)$$

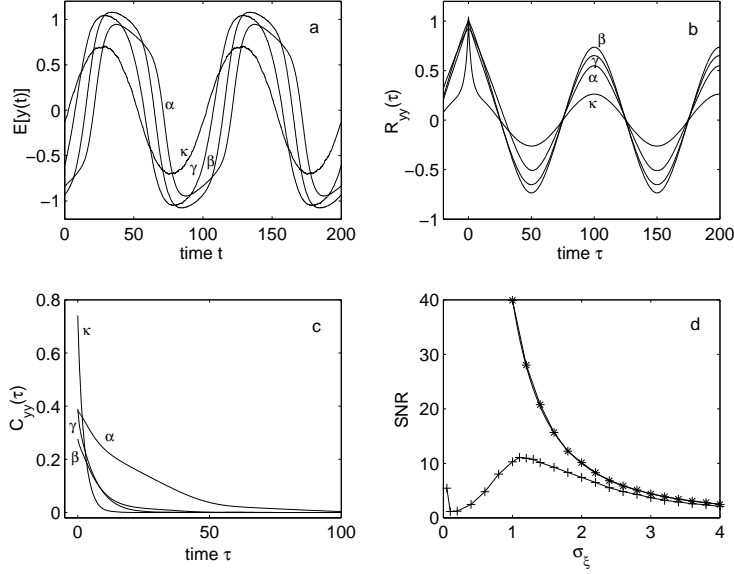


Figure 2: Numerical output behaviors of a single bistable oscillator for $A = 0.4$ at four representative rms amplitudes σ_ξ . (a) The nonstationary mean $E[y(t)]$. (b) The stationary autocorrelation function $R_{yy}(\tau)$. (c) The stationary autocovariance functions $C_{yy}(\tau)$. Here, $\sigma_\xi = 0.6, 1.1, 1.8$ and 3.0 correspond to curves α, β, γ and κ . (d) The theoretical input SNR (solid line) of Eq. (14) as a function of σ_ξ . The numerical input SNR R_{in} (*) but almost indistinguishable) and output SNR R_{out} (+) are also plotted.

In the same way, the periodic sinusoidal input $s(t) = A \sin(2\pi t/T_s)$ has total power $A^2/2$ and power spectral density $A^2[\delta(\nu + 1/T_s) + \delta(\nu - 1/T_s)]/4$ in the context of bilateral power spectral density [31]. Here, the signal-plus-noise mixture of $s(t) + \xi(t)$ is initially given, and the theoretical expression of input SNR can be computed as

$$R_{in}(1/T_s) = \frac{A^2/4}{D_\xi \Delta B} = \frac{A^2/4}{\sigma_\xi^2 \Delta t \Delta B}. \quad (14)$$

In the discrete-time implementation of the white noise, the sampling time $\Delta t \ll T_s$ and τ_a . The incoherent statistical fluctuations in the input $s(t) + \xi(t)$, which controls the continuous noise background in the power spectral density, are measured by the variance $\sigma_\xi^2 = D_\xi/\Delta t$ [31, 33]. Here, σ_ξ is the rms amplitude of input noise $\xi(t)$.

Thus, the array SNR gain, viz. the ratio of the output SNR of array to the input SNR for the coherent component at frequency $1/T_s$, follows as

$$G(1/T_s) = \frac{R_{out}(1/T_s)}{R_{in}(1/T_s)} = \frac{|\bar{Y}_1|^2}{\langle \text{var}[y(t)] \rangle H(1/T_s)} \frac{\sigma_\xi^2 \Delta t}{A^2/4}. \quad (15)$$

Equations (12)–(15) can at best provide a generic theory of evaluating SNR of dynamical systems [31]. If the array SNR gain exceeds unity, the interactions of dynamic array of bistable oscillators and controllable array noise provide a specific potentiality for array signal processing. This possibility will be established in the next sections.

3 Numerical results of array SR and SNR gain

We have carried out the simulation of parallel arrays of Eq. (1) and evaluated the array SNR gain of Eq. (15), as shown in Appendix A, based on the theoretical derivations contained in [31, 33]. Here, we mainly present numerical result as follows.

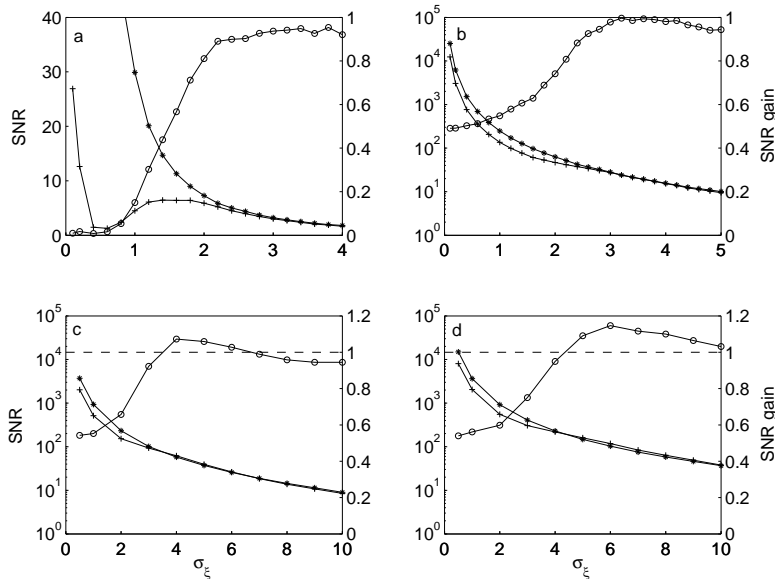


Figure 3: Numerical input SNR R_{in} (*), output SNR R_{out} (+) at the left axes and array SNR gain $G(1/T_s)$ (o) at the right axes, as a function of σ_ξ , in a single bistable oscillator for (a) $A = 0.88A_c \approx 0.34$, (b) $A = 2.6A_c \approx 1.0$, (c) $A = 5A_c \approx 1.925$ and (d) $A = 10A_c \approx 3.849$. Here $T_s = 100$, $\Delta t \Delta B = 10^{-3}$, $\Delta t = T_s \times 10^{-3}$ and $K = 10^5$.

3.1 Improvement of the array SNR gain by noise for array size $N = 1$

If the array size $N = 1$ and the response $y(t) = (1/N) \sum_{i=1}^N x_i(t) = x_1(t)$, this is the case of a single bistable oscillator displaying the conventional SR or residual SR phenomena [1, 20, 21]. In Figs. 2 (a)–(c), we show the evolutions of $E[y(t)]$, $R_{yy}(\tau)$ and $C_{yy}(\tau)$, respectively. The input is a sinusoidal signal with amplitude $A = 0.4$ and frequency $1/T_s = 0.01$ mixed to the noise $\xi(t)$. As the rms amplitude σ_ξ increases, the periodic output mean $E[y(t)]$ has a same frequency $1/T_s = 0.01$, as shown in Fig. 2 (a), and the largest amplitude of $E[y(t)]$ appears at the resonance region around $\sigma_\xi = 1.1$. Plots of the stationary autocovariance function $C_{yy}(\tau)$, as depicted in Fig. 2 (c), indicate that the correlation time τ_r decreases as σ_ξ increases, but the stationary variance $C_{yy}(0) = \langle \text{var}[y(t)] \rangle$ presents a non-monotonic behavior. As σ_ξ increases from 0.6 to 1.1, 1.8 and 3.0, the correlation time τ_r decreases from 65.1 to 27.7, 17.4 and 7.5, whereas $C_{yy}(0)$ equals to 0.383, 0.277, 0.390 and 0.741, respectively. Thus, these nonlinear characteristics of $E[y(t)]$ and $C_{yy}(\tau)$ lead to the SR phenomenon of the output SNR R_{out} versus the rms amplitude σ_ξ in a single bistable oscillator, as illustrated in Fig. 2 (d). The numerical input SNR R_{in} is also plotted in Fig. 2 (d) and agrees well with the theoretical one obtained by Eq. (14). Note that this SR effect is residual SR introduced in Ref. [20], since the amplitude $A = 0.4 > A_c$ is slightly suprathreshold. Similar results are presented in Fig. 3 for subthreshold amplitude ($A = 0.34 < A_c$) and strong suprathreshold ones ($A = 2.6A_c$, $5A_c$ and $10A_c$). Clearly, the SR-type behaviors of R_{out} disappear for strong suprathreshold amplitudes. These numerical results show recurrence of the phenomena of conventional SR [1] and residual SR [20], and show the validity of cyclostationary analysis presented in Sec.2 [31].

The SNR gain $G(1/T_s)$ is also depicted in Fig. 3 at the right axes. It is well known that the SNR gain $G(1/T_s)$ is below unity, so far as the sinusoidal amplitude A is subthreshold or slightly suprathreshold [1, 2, 5, 23, 24, 25], as seen in Fig. 2 (d) and Fig. 3 (a). However, as the amplitude A increases to a more suprathreshold value such as $A = 2.6A_c$, $G(1/T_s)$ approaches unity very closely at $\sigma_\xi = 3.2$, as shown in Fig. 3 (b). Interestingly enough, the possibility of $G(1/T_s)$ exceeding unity exists for strong suprathreshold sinusoidal inputs

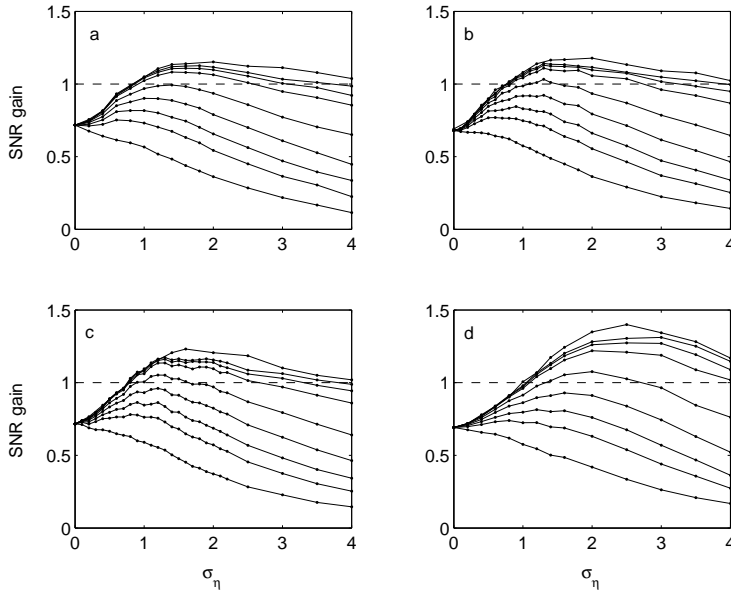


Figure 4: Numerical array SNR gain as a function of the rms amplitude σ_η of array noise $\eta_i(t)$ for (a) $A = 0.34$, (b) $A = 0.38$, (c) $A = 0.4$ and (d) $A = 1.0$. The array SNR gain curves correspond to $N = 1, 2, 3, 5, 10, 30, 60, 120, \infty$ (from the bottom up). The input noise rms amplitudes $\sigma_\xi = 1.8$ for all amplitudes A , with given input SNRs $R_{\text{in}} = 8.92, 11.14, 12.35,$ and 77.16 , respectively. Here $T_s = 100$, $\Delta t \Delta B = 10^{-3}$, $\Delta t = T_s \times 10^{-3}$ and $K = 10^5$.

($A = 5A_c$ or $10A_c$) at certain noise level regimes, as plotted in Figs. 3 (c) and (d). This result is consistent with the work by Hänggi *et al* [2].

These numerical results indicate that this theoretical framework of cyclostationary signal processing in [31] can fully describe the SR phenomena in a single bistable oscillator, and we shall now apply it to the SR effects in parallel uncoupled arrays of bistable oscillators with a noisy sinusoidal input $s(t) + \xi(t)$.

3.2 Improvement by noise of the array SNR gain for array size $N \geq 2$

If the array size $N \geq 2$, this is the case of parallel arrays of bistable oscillators displaying array SR phenomena. Figure 4 displays evolutions of the array SNR gain $G(1/T_s)$ as a function of the rms amplitude σ_η of array noise $\eta_i(t)$, for both subthreshold ($A = 0.34$ and 0.38) and suprathreshold inputs ($A = 0.4$ and 1.0). The input noise rms amplitude is $\sigma_\xi = 1.8$, resulting in the given input SNRs $R_{\text{in}} = 8.92, 11.14, 12.35,$ and 77.16 , respectively. Then, due to array noise $\eta_i(t)$, the array SNR gain $G(1/T_s)$ exhibits nonmonotonic behavior as a function of σ_η for $N \geq 2$. This collective phenomenon can be termed as “array SR” [33], appearing for not only suprathreshold inputs, as shown in Figs. 4 (c) and (d), but also *subthreshold* signals, as presented in Figs. 4 (a) and (b). More importantly, Fig. 4 reveals that the region of the array SNR gain $G(1/T_s)$ raising above unity, via increasing σ_η , is possible for moderately large array size N . Furthermore, as A increases, $G(1/T_s)$ reaches a larger and larger local maximal value for the same N . For instance, $G(1/T_s)$ is about 1.1 for $A = 0.34$ and $N = 120$, as shown in Fig. 4 (a), whereas $G(1/T_s)$ is around 1.3 for $A = 1.0$ and $N = 120$, as seen in Fig. 4 (d).

The mechanism of conventional SR, as shown in Figs. 2–3, exploits a combination of the positive role of input noise $\xi(t)$ and the nonlinearity of a single oscillator [1, 2]. Given a noisy signal, the mechanism of array SR and the possibility of array SNR gains above unity are clearly attributed to the added array noise $\eta_i(t)$ interacting with the nonlinearity of the

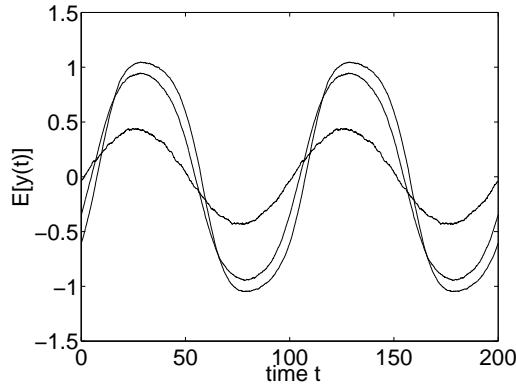


Figure 5: Plots of nonstationary mean $E[y(t)]$ of $y(t)$ for $A = 0.4$ at $\sigma_\eta = 0, 1.3$ and 4.0 (from the top down). $E[y(t)]$ is a periodic function of time t with period $T_s = 100$. Here, $t \in [0, 2T_s[$ and $\Delta t = T_s \times 10^{-3}$.

array [33]. Figure 5 shows that nonstationary means of $E[y(t)]$ are same for $N = 1, 2, \dots, \infty$, at fixed σ_η , since

$$E[y(t)] = E\left[\sum_{i=1}^N x_i(t)/N\right] = \sum_{i=1}^N E[x_i(t)]/N = E[x_i(t)]. \quad (16)$$

However, we note that the amplitude of $E[y(t)]$ decreases as σ_η increases, as shown in Fig. 5. At time t , we have

$$\begin{aligned} R_{yy}(\tau) &= \langle E[y(t)y(t+\tau)] \rangle = \left\langle E\left[\frac{\sum_{i=1}^N x_i(t)}{N} \cdot \frac{\sum_{j=1}^N x_j(t+\tau)}{N}\right]\right\rangle \\ &= \left\langle \frac{E[x_i(t)x_i(t+\tau)]}{N} + \frac{(N-1)E[x_i(t)x_j(t+\tau)]}{N} \right\rangle, \end{aligned} \quad (17)$$

and

$$\begin{aligned} C_{yy}(\tau) &= R_{yy}(\tau) - \langle E[y(t)]E[y(t+\tau)] \rangle = R_{yy}(\tau) - \left\langle \frac{E[\sum_{i=1}^N x_i(t)]E[\sum_{j=1}^N x_j(t+\tau)]}{N^2} \right\rangle \\ &= \left\langle \frac{E[x_i(t)x_i(t+\tau)]}{N} + \frac{(N-1)E[x_i(t)x_j(t+\tau)]}{N} - E[x_i(t)]E[x_j(t+\tau)] \right\rangle, \end{aligned} \quad (18)$$

for $i \neq j$ and $i, j = 1, 2, \dots, N$. Note that $E[x_i(t)] = E[x_j(t)]$.

Figures 6 (a) and (c) show that, at $\sigma_\eta = 1.3$, $R_{yy}(\tau)$ and $C_{yy}(\tau)$ weaken as the array size N increases. On the other hand, for a fixed array size such as $N = 120$, Figs. 6 (b) and (d) suggest that the output behaviors of $R_{yy}(\tau)$ and $C_{yy}(\tau)$ also weaken as σ_η increases from 0 to 1.3 and 4.0. Correspondingly, the stationary variance $C_{yy}(0) = 0.39, 0.25$ and 0.15 , and the correlation time $\tau_r = 17.4, 12.1$ and 4.2 . An association of the time evolutions of $E[y(t)]$ and $C_{yy}(\tau)$ results in SR-type curves of the array SNR gain $G(1/T_s)$ presented in Fig. 4.

3.3 Improvement by noise of the array SNR gain for array size $N = \infty$

Figure 4 shows that the array SNR gain $G(1/T_s)$ is an increasing function of array size N . Thus, it is interesting to know how much the maximal value of $G(1/T_s)$ reaches as array size

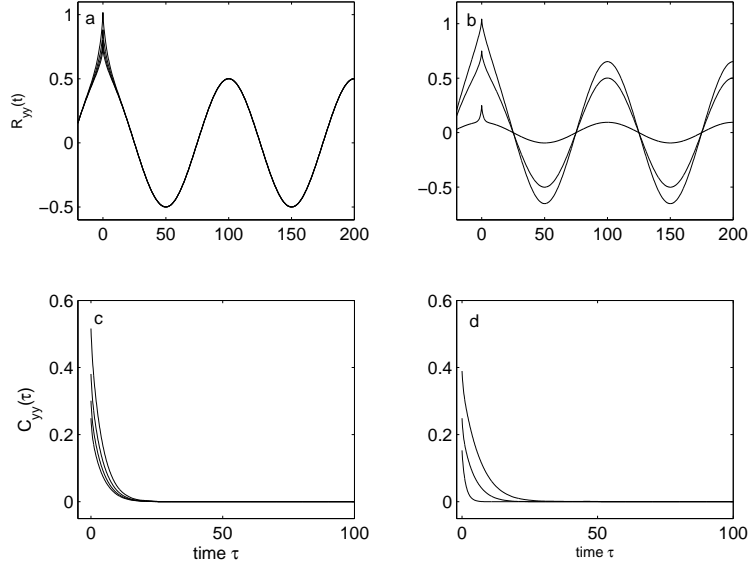


Figure 6: Numerical behaviors of $R_{yy}(\tau)$ and $C_{yy}(\tau)$. (a) $R_{yy}(\tau)$ at $\sigma_\eta = 1.3$ for array sizes $N = 1, 2, 5$ and 120 (from the top down). (b) $R_{yy}(\tau)$ with array size $N = 120$ as σ_η varies from zero to 1.3 and 4.0 (from the top down). (c) $C_{yy}(\tau)$ at $\sigma_\eta = 1.3$ for array sizes $N = 1, 2, 5$ and 120 (from the top down). (d) $C_{yy}(\tau)$ with array size $N = 120$ as σ_η changes from zero to 1.3 and 4.0 (from the top down). Here, $A = 0.4$, and other parameters are the same as in Fig. 4.

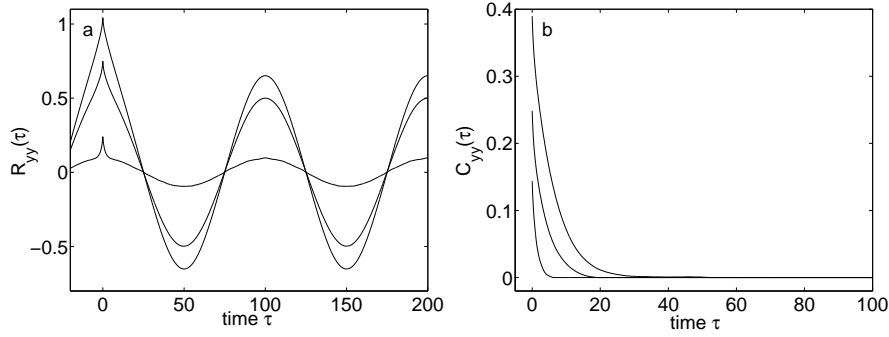


Figure 7: Numerical output behaviors of arrays for array size $N = \infty$. (a) $R_{yy}(\tau)$ and (b) $C_{yy}(\tau)$ as functions of $\sigma_\eta = 0, 1.3$ and 4.0 (from the top down). Other parameters are the same as in Fig. 4.

$N = \infty$. Form Eqs. (17) and (18), we have [43]

$$\begin{aligned}
\lim_{N \rightarrow \infty} R_{yy}(\tau) &= \lim_{N \rightarrow \infty} \langle E[y(t)y(t+\tau)] \rangle \\
&= \lim_{N \rightarrow \infty} \left\langle \frac{E[x_i(t)x_i(t+\tau)] + (N-1)E[x_i(t)x_j(t+\tau)]}{N} \right\rangle \\
&= \langle E[x_i(t)x_j(t+\tau)] \rangle \\
&= R_{x_i x_j}(\tau),
\end{aligned} \tag{19}$$

and

$$\begin{aligned}
\lim_{N \rightarrow \infty} C_{yy}(\tau) &= \lim_{N \rightarrow \infty} R_{yy}(\tau) - \lim_{N \rightarrow \infty} \langle E[y(t)]E[y(t+\tau)] \rangle \\
&= \lim_{N \rightarrow \infty} R_{yy}(\tau) - \lim_{N \rightarrow \infty} \left\langle \frac{E[\sum_{i=1}^N x_i(t)]E[\sum_{j=1}^N x_j(t+\tau)]}{N^2} \right\rangle \\
&= \langle E[x_i(t)x_j(t+\tau)] \rangle - \langle E[x_i(t)]E[x_j(t+\tau)] \rangle \\
&= C_{x_i x_j}(\tau),
\end{aligned} \tag{20}$$

for $i \neq j$ and $i, j = 1, 2, \dots, N$. Since the indices i and j are different, but arbitrary in Eqs. (19) and (20), we can adopt two bistable oscillators, each embedded with independent noise, to evaluate the array SNR gain of a parallel array with size $N = \infty$. The behaviors of $R_{yy}(\tau)$ and $C_{yy}(\tau)$ are plotted in Fig. 7 as the rms amplitude σ_η increases from 0, 1.3 to 4.0. The stationary variance $C_{yy}(0) = 0.39, 0.25$ and 0.15 , and the correlation time $\tau_r = 17.2, 12.1$ and 4.2 , respectively. Furthermore, the output SNR R_{out} of a parallel array of bistable oscillators with infinite size $N = \infty$ is obtained from Eq. (12), and same for the array SNR gain $G(1/T_s)$ of Eq. (15). Numerical results of $G(1/T_s)$ are also plotted in Fig. 4 as $N = \infty$.

From Figs. 4–7, the mechanism of array SR and the possibility of array SNR gain above unity can be explained by the fact that independent array noise, on the one hand, help the array response to reach its mean $E[y(t)]$, on the other hand, counteract the negative role of input noise and ‘whiten’ the output statistical fluctuations $\tilde{y}(t)$. In other words, the stationary autocovariance function $C_{yy}(\tau)$ has a decreasing stationary variance $C_{yy}(0)$ and correlation time τ_r , as shown in Figs. 6 and 7.

4 Optimization of the array SNR gain of an infinite array

For a given input noisy signal and a fixed array size N , there is a local maximal SNR gain, i.e. the maximum value of $G(1/T_s)$ at the SR point of rms amplitude σ_η of array noise, as shown in Fig. 4. Clearly, this local maximal SNR gain increases as array size N increases, and arrives at its global maximum $G_{\text{max}}(1/T_s)$ as $N = \infty$. Note that $G_{\text{max}}(1/T_s)$ is obtained only via adding array noise $\eta_i(t)$. It is interesting to know if $G_{\text{max}}(1/T_s)$ can be improved further by tuning both array noise $\eta_i(t)$ and the array parameter X_b .

In Eq. (3), the signal amplitude $A/X_b \rightarrow A$ is dimensionless, and the discrete implementation of noise results in the dimensionless rms amplitude of $\sigma_\xi/X_b \rightarrow \sigma_\xi$ or $\sigma_\eta/X_b \rightarrow \sigma_\eta$ (where each arrow points to a dimensionless variable). The dimensionless ratio of A/σ_ξ , as $\Delta t \Delta B = 10^{-3}$, determines the input SNR R_{in} of Eq. (14). In Fig. 8, we adopt two given input SNRs $R_{\text{in}} = 40$ and 10 , this is, $A/\sigma_\xi = 0.4$ and 0.2 . When the array parameter X_b varies, but A/σ_ξ keeps, line L_1 comes into being, and is divided into subthreshold region ($A < 2/\sqrt{27}$) and suprathreshold regime ($A > 2/\sqrt{27}$) by line L_2 of $A = 2/\sqrt{27}$, as shown in Figs. 8 (a) and (c). We select different points on line L_1 , being located in subthreshold region or suprathreshold region, for computing $G_{\text{max}}(1/T_s)$ via increasing σ_η , as illustrated in Figs. 8 (b) and (d). Figure 8 (b) shows that, at the given input SNR $R_{\text{in}} = 40$, the global maximum SNR gain $G_{\text{max}}(1/T_s)$ increases from low amplitude $A = 0.25$, i.e. point P_1 , reaches its maximum around $\sigma_\eta = 2.0$ for $A = 0.38$, i.e. point P_4 , then gradually decreases

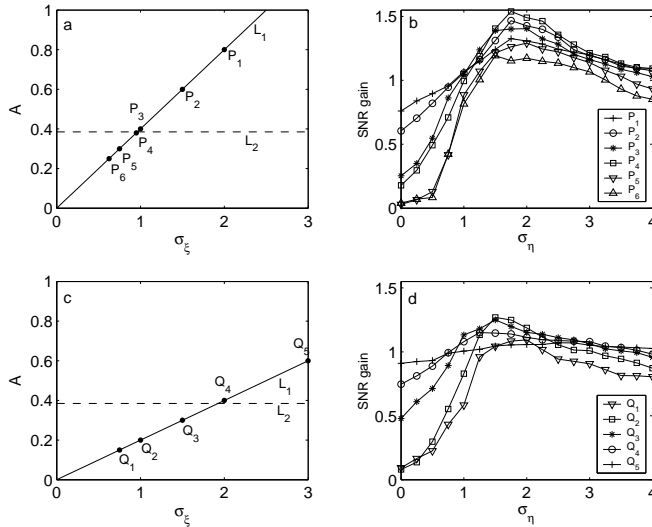


Figure 8: (a) Plots of amplitude A versus input noise rms amplitude σ_ξ (dimensionless variables). Line L_1 is $A/\sigma_\xi = 0.4$, and the corresponding input SNR $R_{\text{in}} = 40$. Line L_2 of $A = 2/\sqrt{27} \approx 0.385$ divides line L_1 into subthreshold region (below L_2) and suprathreshold section (over L_2). Points P_i ($i = 1, 2, \dots, 6$) correspond to $A = 0.8, 0.6, 0.4, 0.38, 0.3$ and 0.25 , respectively. (b) The global maximum SNR gain $G_{\text{max}}(1/T_s)$, at fixed input SNR $R_{\text{in}} = 40$, as a function of rms amplitude σ_η of array noise for points P_i (different amplitudes A). (c) Plots of A versus σ_ξ . Line L_1 is $A/\sigma_\xi = 0.2$, and $R_{\text{in}} = 10$. Line L_2 is $A = 2/\sqrt{27}$. Points Q_i ($i = 1, 2, \dots, 5$) correspond to $A = 0.15, 0.2, 0.3, 0.4$ and 0.6 , respectively. (d) $G_{\text{max}}(1/T_s)$, at $R_{\text{in}} = 10$, as a function of σ_η for points Q_i . Here, $T_s = 100$, $\Delta B = 1/T_s$ and $\Delta t \Delta B = 10^{-3}$.

as the amplitude A increases to 0.8 (point P_1). The same effect occurs for the given input SNR $R_{\text{in}} = 10$, as shown in Fig. 8 (d), and $A = 0.2$ (point Q_2) corresponds to the maximum $G_{\text{max}}(1/T_s)$ around $\sigma_\eta = 1.5$. These results indicate that, for a given input SNR, we can tune the array parameter X_b to an optimal value, corresponding to an optimized global maximum SNR gain.

However, we do not consider the other array parameter τ_a , which is associated with the time scale of temporal variables [21]. Then, the location of optimal array parameters X_b in subthreshold or suprathreshold regions, associated with optimal σ_η , is pending. Immediately, an open problem, optimizing the global maximum SNR gain $G_{\text{max}}(1/T_s)$ via tuning array parameters (X_b and τ_a) and adding array noise (increasing σ_η), is very interesting but time-consuming. This paper mainly focuses on the demonstration of a situation of array signal processing where the parallel array of dynamical systems can achieve a maximum SNR gain above unity via the addition of array noise. Thus, the optimization of the maximum SNR gain of infinite array is touched upon, and this interesting open problem will be considered in future studies.

5 Conclusions

In the present work we concentrated on the SNR gain in parallel uncoupled array of bistable oscillators. For a mixture of sinusoidal signal and Gaussian white noise, we observe that the array SNR gain does exceed unity for both subthreshold and suprathreshold signals via the addition of mutually independent array noise. This frequently confronted case of a given noisy input and controllable fact of array noise make the above observation interesting in array signal processing.

We also observe that, in the configuration of the present parallel array, the array SNR gain displays a SR-type behavior for array size larger than one, and increases as the array size rises for a fixed input SNR. This SR-type effect of the array SNR gain, i.e. array SR, is distinct from other SR phenomena, in the view of occurring for both subthreshold and suprathreshold signals via the addition of array noise. The mechanism of array SR and the possibility of array SNR gain above unity were schematically shown by the nonstationary mean and the stationary autocovariance function of array collective responses.

Since the global maximum SNR gain is always achieved by an infinite parallel array at non-zero added array noise levels, we propose a theoretical approximation of an infinite parallel array as an array of two bistable oscillators, in view of the functional limit of the autocovariance function. Combined with controllable array noise, this nonlinear collective characteristic of parallel dynamical arrays provides an efficient strategy for processing periodic signals.

We argue that, for a given input SNR, tuning one array parameter can optimize the global maximum SNR gain at an optimal array noise intensity. However, another array parameter, associated with the time scale of temporal variables is not involved. An open problem, optimizing the global maximum SNR gain via tuning two array parameters and array noise, is interesting and remains open for future research.

6 Acknowledgment

Funding from the Australian Research Council (ARC) is gratefully acknowledged. This work is also sponsored by ‘‘Taishan Scholar’’ CPSP, NSFC (No. 70571041), the SRF for ROCS, SEM and PhD PFME of China (No. 20051065002).

A Numerical method of computing power spectra of the collective response of arrays

The corresponding measured power spectra of the collective response $y(t) = (1/N) \sum_{i=1}^N x_i(t)$ are computed in a numerical iterated process in the following way that is based on the theoretical derivations contained in [31, 33]: The total evolution time of Eq. (1) is $(K + 1)T_s$, while the first period of data is discarded to skip the start-up transient [29, 2]. In each period T_s , the time scale is discretized with a sampling time $\Delta t \ll T_s$ such that $T_s = L\Delta t$. The white noise is with a correlation duration much smaller than T_s and Δt . We choose a frequency bin $\Delta B = 1/T_s$, and we shall stick to $\Delta t \Delta B = 10^{-3}$, $T_s = 100$, $L = 1000$ and $K \geq 10^5$ for the rest of the paper. In succession, we follow:

(a) The estimation of the mean $E[y(j\Delta t)]$ is obtained over one period $[0, T_s[$, and the precise time $j\Delta t$ of $E[y(j\Delta t)]$ ($j = 0, 1, \dots, L-1$) shall be tracked correctly in each periodic evolution of Eq. (1), i.e. $[kT_s, (k+1)T_s[$ for $k = 1, 2, \dots, K$.

(b) For a fixed time of $\tau = i\Delta t$ ($i = 0, 1, \dots, \tau_{\max}/\Delta t$), the products $y(j\Delta t)y(j\Delta t + i\Delta t)$ are calculated for $j = 1, 2, \dots, KT_s/\Delta t$. The estimation of the expectation $E[y(j\Delta t)y(j\Delta t + i\Delta t)]$ is then performed. From Eq. (8), the stationary autocorrelation function $R_{yy}(\tau)$ can be estimated over a time domain $\tau \in [0, \tau_{\max}[$. Immediately, the stationary autocovariance function $C_{yy}(i\Delta t)$ of Eq. (8) at $i = 0, 1, \dots, \tau_{\max}/\Delta t$ can be deduced. Note the time τ_{\max} is selected in such a way that at τ_{\max} , the stationary autocovariance function $C_{yy}(i\Delta t)$ in Eq. (8) has returned to zero. In practice, we can select a quite small positive real number ε , such as $\varepsilon = 10^{-5}$. If $C_{yy}(i\Delta t)/C_{yy}(0) \leq \varepsilon$, the above computation shall be ceased and the index i_{end} is found, leading to $\tau_{\max} = i_{\text{end}}\Delta t$.

(c) Increase the total evolution time of Eq. (1) as $(K' + 1)T_s$ ($K' > K$), and evaluate the mean $E'[y(j\Delta t)]$ and the stationary autocovariance function $C'_{yy}(i\Delta t)$ again. If the differences between $E'[y(j\Delta t)]$ and $E[y(j\Delta t)]$, $C'_{yy}[i\Delta t]$ and $C_{yy}(i\Delta t)$, converged within an allowable tolerance, we go to the next step (d). If they do not converge, the total evolution time of Eq. (1) should be increased to $(K'' + 1)T_s$ larger than $(K' + 1)T_s$, until the convergence is realized.

(d) With the converged mean $E[y(j\Delta t)]$ and stationary autocovariance function $C_{yy}(i\Delta t)$, the corresponding Fourier coefficient \bar{Y}_1 and the power $\overline{\text{var}[y(t)]}H(1/T_s)\Delta B$ of Eq. (8) contained in the noise background around $1/T_s$ can be numerically developed. The ratio of above numerical values leads to the array SNR R_{out} . The correlation time $\tau_r = M\Delta t$ as $|h(M\Delta t)| = |C_{yy}(M\Delta t)/C_{yy}(0)| \leq 0.05$. The numerical input SNR R_{in} can be also calculated by following steps (a)–(d), and compared with the theoretical value of R_{in} of Eq. (13). The SNR gain $G(1/T_s)$ will be finally figured out by Eq. (15).

References

- [1] L. Gammaitoni, P. Hänggi, P. Jung, and F. Marchesoni, Stochastic resonance, *Rev. Mod. Phys.*, **70**, pp. 233-287 (1998).
- [2] P. Hänggi, M. Inghiosa, D. Fogliatti, and A.R. Bulsara, Nonlinear stochastic resonance: The saga of anomalous output-input gain, *Phys. Rev. E*, **62**, pp. 6155-6163 (2000).
- [3] J.J. Collins, C.C. Chow, and T.T. Imhoff, Aperiodic stochastic resonance in excitable systems, *Phys. Rev. E*, **52**, pp. R3321-R3324 (1995).
- [4] M.E. Inghiosa, and A.R. Bulsara, Signal detection statistics of stochastic resonators, *Phys. Rev. E*, **53**, pp. R2021-R2024 (1996).
- [5] M.E. Inghiosa, and A.R. Bulsara, Nonlinear dynamic elements with noisy sinusoidal forcing: Enhancing response via nonlinear coupling, *Phys. Rev. E*, **52**, pp. 327-339 (1995).
- [6] J.F. Lindner, B.K. Meadows, W.L. Ditto, M.E. Inghiosa, and A.R. Bulsara, Array enhanced stochastic resonance and spatiotemporal synchronization, *Phys. Rev. Lett.*, **75**, pp. 3-6 (1995).
- [7] J.M. Casado, J. Gómez-Ordóñez, and M. Morillo, Stochastic resonance of collective variables in finite sets of interacting identical subsystems, *Phys. Rev. E*, **73**, 011109 (2006).
- [8] P. Jung, and G. Mayer-Kress, Spatiotemporal stochastic resonance in excitable media, *Phys. Rev. Lett.*, **74**, pp. 2130-2133 (1995).
- [9] J.J. Collins, C.C. Chow, and T.T. Imhoff, Stochastic resonance without tuning, *Nature*, **376**, pp. 236-238 (1995).
- [10] D.R. Chialvo, A. Longtin, and J. Müller-Gerking, Stochastic resonance in models of neuronal ensembles, *Phys. Rev. E*, **55**, pp. 1798-1808 (1997).
- [11] F. Moss, and X. Pei, Neurons in parallel, *Nature*, **376**, pp. 211-212 (1995).
- [12] N.G. Stocks, Suprathreshold stochastic resonance in multilevel threshold systems, *Phys. Rev. Lett.*, **84**, pp. 2310-2313 (2000).
- [13] N.G. Stocks, Suprathreshold stochastic resonance: an exact result for uniformly distributed signal and noise, *Phys. Lett. A*, **279**, pp. 308-312 (2001).
- [14] N.G. Stocks, Information transmission in parallel threshold arrays: Suprathreshold stochastic resonance, *Phys. Rev. E*, **63**, 041114 (2001).
- [15] N.G. Stocks, and R. Mannella. Generic noise-enhanced coding in neuronal arrays, *Phys. Rev. E*, **64**, 030902(R) (2001).
- [16] N.G. Stocks, D. Allingham, and R.P. Morse, The application of suprathreshold stochastic resonance to cochlear implant coding, *Fluctuation and Noise Lett.*, **2**, pp. L169-L181 (2002).

- [17] M.D. McDonnell, D. Abbott, and C.E.M. Pearce, A characterization of suprathreshold stochastic resonance in an array of comparators by correlation coefficient, *Fluctuation and Noise Lett.*, **2**, pp. L213-L228 (2002).
- [18] M.D. McDonnell, N.G. Stocks, C.E.M. Pearce, and D. Abbott, Optimal information transmission in nonlinear arrays through suprathreshold stochastic resonance, *Phys. Lett. A*, **352**, pp. 183-189 (2006).
- [19] D. Rousseau, and F. Chapeau-Blondeau, Suprathreshold stochastic resonance and signal-to-noise ratio improvement in arrays of comparators, *Phys. Lett. A*, **321**, pp. 280-290 (2004).
- [20] F. Apostolico, L. Gammaitoni, F. Marchesoni and S. Santucci. Resonant trapping: A failure mechanism in switch transitions. *Phys. Rev. E*, **55**, pp. 36-39 (1997).
- [21] F. Duan, D. Rousseau, and F. Chapeau-Blondeau, Residual aperiodic stochastic resonance in a bistable dynamic system transmitting a suprathreshold binary signal, *Phys. Rev. E*, **69**, 011109 (2004).
- [22] G. Debnath, T. Zhou, and F. Moss, Remarks on stochastic resonance, *Phys. Rev. A*, **39**, pp. 4323-4326 (1989).
- [23] P. Jung and P. Hänggi, Amplification of small signals via stochastic resonance, *Phys. Rev. A*, **44**, pp. 8032-8042 (1991).
- [24] M.I. Dykman, and P.V.E. McClintock, What can stochastic resonance do? *Nature*, **391**, pp. 344 (1998).
- [25] M.I. Dykman, R. Mannella, P.V.E. McClintock, and N.G. Stocks, Fluctuation-induced transitions between periodic attractors: Observation of supernarrow spectral peaks near a kinetic phase transition, *Phys. Rev. Lett.*, **65**, pp. 48-51 (1990).
- [26] A. Neiman, L. Schimansky-Geier, and F. Moss, Linear response theory applied to stochastic resonance in models of ensembles of oscillators, *Phys. Rev. E*, **56**, pp. R9-R12 (1997).
- [27] P.C. Gailey, A. Neiman, J.J. Collins, and F. Moss, Stochastic resonance in ensembles of nondynamical elements: The role of internal noise, *Phys. Rev. Lett.*, **79**, pp. 4701-4704 (1997).
- [28] K. Loerincz, Z. Gingl, and L.B. Kiss, A stochastic resonator is able to greatly improve signal-to-noise ratio, *Phys. Lett. A*, **224**, pp. 63-67 (1996).
- [29] F. Chapeau-Blondeau, Input-output gains for signal in noise in stochastic resonance, *Phys. Lett. A*, **232**, pp. 41-48 (1997).
- [30] F. Chapeau-Blondeau, Periodic and aperiodic stochastic resonance with output signal-to-noise ratio exceeding that at the input, *Int. J. Bifurcation and Chaos*, **9**, pp. 267-272 (1999).
- [31] F. Chapeau-Blondeau, and X. Godivier, Theory of stochastic resonance in signal transmission by static nonlinear systems, *Phys. Rev. E*, **55**, pp. 1478-1495 (1997).
- [32] F. Chapeau-Blondeau, and D. Rousseau, Enhancement by noise in parallel arrays of sensors with power-law characteristics, *Phys. Rev. E*, **70**, 060101(R) (2004).
- [33] F. Chapeau-Blondeau, and D. Rousseau, Noise-aided SNR amplification by parallel arrays of sensors with saturation, *Phys. Lett. A*, **351**, pp. 231-237 (2006).
- [34] Z. Gingl, R. Vajtai, and L.B. Kiss, Signal-to-noise gain by stochastic resonance in a bistable system, *Chaos, Solitons and Fractals*, **11**, pp. 1929-1932 (2000).

- [35] Z. Gingl, P. Makra, and R. Vajtai, High signal-to-noise ratio gain by stochastic resonance in a double well, *Fluctuation and Noise Lett.*, **1**, pp. L181-L188 (2001).
- [36] J. Casado-Pascual, J. Gómez-Ordóñez, and M. Morillo, Two-state theory of nonlinear stochastic resonance, *Phys. Rev. Lett.*, **91**, 210601 (2003).
- [37] J. Casado-Pascual, C. Denk, J. Gómez-Ordóñez, and M. Morillo, Gain in stochastic resonance: Precise numerics versus linear response theory beyond two-mode approximation, *Phys. Rev. E*, **67**, 036109 (2003).
- [38] J. Casado-Pascual, J. Gómez-Ordóñez, M. Morillo, and P. Hänggi, Subthreshold stochastic resonance: Rectangular signals can cause anomalous large gains, *Phys. Rev. E*, **68**, 061104 (2003).
- [39] V.N. Chizhevsky, and G. Giacomelli, Improvement of signal-to-noise ratio in a bistable optical system: Comparison between vibrational and stochastic resonance, *Phys. Rev. A*, **71**, 011801(R) (2005).
- [40] M.E. Inchiosa, A.R. Bulsara, A.D. Hibbs, and B.R. Whitecotton, Signal enhancement in a nonlinear transfer characteristic, *Phys. Rev. Lett.*, **80**, pp. 1381-1384 (1998).
- [41] W.B. Davenport, Signal-to-noise ratios in band-pass limiters, *J. Applied Physics*, **24**, pp. 720-727 (1953).
- [42] B. Xu, F. Duan, and F. Chapeau-Blondeau, Comparison of aperiodic stochastic resonance in a bistable system by adding noise and tuning system parameters, *Phys. Rev. E*, **69**, 061110 (2004).
- [43] F. Duan, F. Chapeau-Blondeau, and D. Abbott, Noise-enhanced SNR gain in parallel array of bistable oscillators, *Electronics Lett.*, **42**, pp. 1008-1009 (2006).